Chemical Physics Letters 712 (2018) 44–53

Contents lists available at ScienceDirect

Chemical Physics Letters

journal homepage: www.elsevier.com/locate/cplett

Research paper

# A reliable approach for calculating thermophysical properties of liquid using molecular dynamics simulations

Seyed Aliakbar Mirmohammadi, Luming Shen*, Yixiang Gan

*School of Civil Engineering, The University of Sydney, NSW 2006, Australia*

## HIGHLIGHTS

- Thermophysical properties of water are evaluated with equilibrium molecular dynamics.
- Deficiency in the conventional data processing method is investigated.
- New data processing method is developed to ensure the reliability of the obtained properties.
- Criterion is introduced to determine the minimum domain size under given conditions.

## ARTICLE INFO

*Keywords:*
Molecular dynamics simulation
Thermophysical properties
Water model
Green-Kubo Method
Data processing

## ABSTRACT

This paper presents a new data processing method for calculating more reliable thermophysical properties of liquid using Green-Kubo Method based molecular dynamics (MD) simulation. In this study, MD simulations of water are first performed using three common water models. A new approach for analysing the simulation data is then developed to obtain statistically meaningful thermophysical properties such as thermal conductivity and viscosity. It is demonstrated that for a given desired standard deviation for a specific simulation, a suitable simulation box size can be determined. The proposed approach can assure the repeatability and reliability of the calculated thermophysical properties of liquid.

## 1. Introduction

During the past few decades, the transport phenomena of liquids have been of great interest in a wide variety of applications. For example, miniaturized systems such as nano-electromechanical systems (NEMS) technology [1] and nanofluids [2–5] have received considerable attentions more recently. Transport properties, such as thermal conductivity and viscosity, serve as the most significant characteristics of materials in thermal studies [6–8]. Hence, accurate measurement of thermophysical properties of liquid plays a critical role in the functionality of NEMS and nanofluids.

Water is the most investigated liquid in the literature due to its widespread use and ubiquity in our environment. Several experimental and numerical methods have been developed to estimate its thermophysical properties. For example, Duangthongsuk and Wongwises applied transient hot-wire apparatus and Bohlin rotational rheometer to measure thermal conductivity and viscosity of water-based nanofluid, respectively [9]. In their study, before the thermophysical properties of nanofluid were measured, the thermophysical properties of the base fluid (pure water) were measured to validate the experimental apparatuses. However, in many cases, experimental measurement can only provide limited insight into the mechanism of thermophysical properties change as a function of certain parameters. As a result, computer simulations have been carried out in order to better understand the properties of mixed molecules and the microscopic interactions between them. A variety of modelling techniques have been developed for calculating the thermophysical properties over the years [10–12]. Among them, molecular dynamics (MD) approach can provide detailed atomic-level information and has been widely employed in many numerical simulation studies on the thermophysical properties of liquids [13–15].

MD simulations for calculating thermophysical properties of liquids could be categorized into two types namely non-equilibrium molecular dynamics (NEMD) [16,17] and equilibrium molecular dynamics (EMD) [18]. In EMD, the system is in equilibrium when the properties are evaluated whereas an external field drives the system away from thermodynamic equilibrium in NEMD. In order to calculate thermophysical properties in EMD simulation, fluctuation-dissipation and

---

* Corresponding author.
*E-mail address:* luming.shen@sydney.edu.au (L. Shen).

https://doi.org/10.1016/j.cplett.2018.09.048
Received 21 June 2018; Accepted 23 September 2018

linear response theorem are usually applied. In contrast, In the NEMD simulations, an external field such as shear force or heat flux needs to be applied to create shear flow or temperature gradient, respectively. Then, the desired properties are monitored and calculated. In a comparative study by Schelling et al. [19], it has been concluded that the EMD approach has considerable advantages over the NEMD approach. Firstly, although both EMD and NEMD approaches show finite size effects, these effects are more severe in NEMD. Secondly, EMD is more appropriate for geometries where periodic boundary conditions are applied in all three directions. On the contrary, NEMD could only accomplish the calculations in one direction. Hence, EMD simulation is applied in this study.

In EMD simulation, Green-Kubo (GK) method, introduced by Green [20] and Kubo [21], has been well-established and widely used for calculating thermophysical properties of liquids. This method is based on Green-Kubo formalism where thermal conductivity or viscosity is calculated by integrating over time of the ensemble average of the autocorrelation of the external field [22].

On the other hand, the most critical part of a molecular dynamics simulation is the potential models. So far, many water models have been developed in order to study the structure and properties of water at the atomic scale. According to a report by Guillot [23], water models are classified into four main types, namely rigid, flexible, dissociable, and polarizable. It has been a matter of discussion that which model may reproduce the most accurate and reliable results in MD simulation of thermophysical properties. However, the answer to this question is not very clear so far as each water potential model was developed to reproduce certain properties under given conditions. In this regard, there are scarcely published studies that compare the performance of different models on reproducing thermophysical properties. For example, González and Abascal [24] calculated the shear viscosity using Green–Kubo method in order to compare five rigid water models including TIP3P [25], TIP4P [25], TIP5P [26], SPC/E[27] and TIP4P/2005 [28]. In a broader study, thermal conductivity, viscosity and specific heat of various rigid water models were calculated and compared with each other using MD simulation [29]. The authors showed that recent developed models, such as TIP5P, are capable of illustrating more accurate values compared with conventional ones.

Moreover, we have noticed that the common data collection method of predicting thermal conductivity and viscosity of liquids using MD simulation is questionable. Take the method used in [18,30,31] for example, when the values of thermal conductivity or viscosity somehow converged after a certain period of production run time, the MD simulation stopped. Then, the values of the thermal conductivity or viscosity in the three directions were recorded. The average value of the properties in the three directions was worked out and presented as the calculated thermal conductivity or viscosity. There were some similar studies, such as the water model comparative study carried out by Mao and Zhang [29], in which the standard deviations of certain thermophysical properties were reported in Tables 3 and 4 of their paper. However, it was not clearly explained how these statistical values were calculated. Also, thermal conductivity of the supercooled water is estimated using GK equation by English and Tse [32]. They did not describe their data collection approach in detail. However, their MD simulation resulted in an uncertainty. In particular, the standard deviation of their calculated thermophysical properties was three times greater than that from the experimental measurement. Similarly, in many other available studies in the literature, data collection procedure has not been clearly described, as the focus of those studies such as [17,33,34] was more on the results reporting and discussion. In addition, Kumar et al. [34] stated that the applied data collection and processing method in their study suffers from poor convergence even for extremely long simulations.

It appears that the common data collection method does not consider the effects of simulation box size, initial conditions, thermostat effectiveness, data sampling frequency, etc., on the simulated thermophysical properties. However, it has been known that these parameters could have significant effects on the results of MD simulations. For example, the MD simulation box size affected the simulated mechanical properties of the nano-material [35]. The simulations were also dependent on the initial conditions that could be changed by using different random number seed. As a result, sufficient number of independent simulations must be carried out and average values of the simulated results should be used in order to obtain reliable results [36]. Hence, a new approach that can produce reliable and repeatable results with controllable standard deviations should be developed.

An intrinsic problem associated with the GK calculation is the artificial correlations. The common method of mitigating the problem is to choose a system size large enough to minimize these correlations. Recently, Muraleedharan et al. [37] tried to mitigate the problem for multicomponent systems (Solid particles immersed in a base fluid) by increasing the number of particles. They observed that adding more particles is likely to hamper the development of the artificial self-correlations. In either method, researchers normally find the proper size or number of particles by trial and error and there are no clear quantified criteria to select an appropriate simulation domain size or particle numbers. Thus, we believe it is important to find a quantifiable data processing method to ensure the reliability and accuracy of the simulated properties.

In the present study, a common problem of MD simulation is considered and a new reliable data-processing approach is developed. In addition, by using the new approach, a criterion in accordance with the standard deviation of the simulation results is introduced. This criterion can be used to select the appropriate size of the system based on the level of the accuracy that is desired for a given simulation. Without the loss of generality, three common rigid water models including SPCE, TIP3P, and TIP4P-2005 will be used at different temperatures and the data collection procedure on the reliability of the simulated thermal conductivity and viscosity of water will be investigated. It is shown that the proposed data collection and processing method is able to effectively control the standard deviation of the simulated values and thus produce reliable and repeatable thermophysical properties from MD simulations.

## 2. Methodology

In this section, the method of calculating thermal conductivity and viscosity by employing Green-Kubo method based EMD simulation will be first described. Then, a new data collection and processing method will be introduced for calculating thermophysical properties of water using MD simulations.

### 2.1. Thermal conductivity

When a liquid system is in equilibrium, it has a constant average temperature and an average heat flux of zero over a finite time period. However, the temperature fluctuates instantaneously, and as a result, a finite heat flux exists at each instant of time [38]. This phenomenon is the base of the Green-Kubo method to calculate thermal conductivity and viscosity in EMD simulation.

In macroscopic scale study, thermal conductivity $k$ is a coefficient that relates the macroscopic heat current vector (**J**) to the temperature (T) gradient in the form of Fourier's law [39]:

$$\overrightarrow{j} = -k\hat{A}\cdot\overrightarrow{\Delta T} \tag{1}$$

However, in microscopic scale study, in order to calculate the thermal conductivity $k$ using EMD simulation, Green-Kubo (GK) method relates the lattice thermal conductivity of the system to the integral of the average of the time correlation function of the heat current through the following relation [21,40]:

$$k = \frac{1}{3Vk_B T^2}\int_0^\infty \langle \vec{j}(t)\cdot\vec{j}(0)\rangle dt \tag{2}$$

where $\vec{j}(t)$ and)$\vec{j}(0)$are the instantaneous microscopic heat current vectors at time *t* and time zero, respectively. Heat flux is calculated using three different fluctuation modes carried by kinematic energy, potential energy, and energy from the collision of atoms. The angular bracket denotes autocorrelation function, *V* is the volume, and $K_B$ is Boltzman's constant. The integral calculates the heat autocorrelation function (HACF) using the time needed for the HACF to decay to zero. More details about Green-Kubo method can be found in [19].

### 2.2. Viscosity

To calculate the viscosity, the same methodology is used as the previous section. However, the heat autocorrelation is replaced by the stress (pressure) autocorrelation function (SACF) in Green-Kubo equation. The time needed for SACF to decay to zero is then used through the Green–Kubo relation to predict the viscosity [41] as given below:

$$\eta = \frac{V}{k_B T}\int_0^t \langle P_{XY}(0)P_{XY}(t)\rangle dt \tag{3}$$

where η is the shear viscosity, V and T are the volume and temperature of the system, respectively, and $P_{XY}$ refers to an independent component of the shear stress in the XY direction. However, for an isotropic, homogeneous fluid in the absence of external fields, the symmetry of the cubic simulation box implies that the three directions X, Y and Z are equivalent in this equation. As a result, all three independent off-diagonal elements of the stress tensor are used in the calculation [42].

### 2.3. Simulation procedures and post-processing of data

Fig. 1(a) shows the cubic simulation box with periodic boundary condition in all three directions, where L represents the box size. Three common water models including SPCE, TIP3P, and TIP4P/2005 were used to study the effect of potential models on the calculated thermophysical properties of water. For each water model, four different simulation box sizes, L = 2 nm, 5 nm, 10 nm or 15 nm, were considered.

Among these three models, SPCE and TIP3P are 3-site model, while TIP4P/2005 is a 4-site model. As can be seen from Fig. 1(b), the 3-site model only consists of two hydrogen (H) atoms and 1 oxygen (O) atom (the upper configuration), while the 4-site model has an extra dummy atom (M) shown as a [1]yellow sphere (the lower configuration), which has charge of −1.1128e. Table 1 reports the charge of H, O and M atoms, the O—H (r (OH)) and O—M (r (OM)) bond lengths, and the H-O—H angle of each water model. In all the MD simulations, angles and bond lengths are kept rigid. Two other parameters σ and ε are referred to the Lennard-Jones potential that describes the O—O interaction between two different water molecules. All potential functions of rigid water molecules consist of the contributions from electrostatic, dispersion and repulsive forces as demonstrated in the equation below:

$$E_{ab} = \sum_{i}^{ona}\sum_{j}^{onb}\frac{K_C q_{a_i} q_{b_j}}{r_{a_i b_j}} + \sum_{i}^{ona}\sum_{j}^{onb} 4\varepsilon_{a_i b_j}\left[\left(\frac{\sigma_{a_i b_j}}{r_{a_i b_j}}\right)^{12} - \left(\frac{\sigma_{a_i b_j}}{r_{a_i b_j}}\right)^{6}\right] \tag{4}$$

where subscript i and j denote atoms i and j in one individual molecule for SPCE and TIP3P water molecules in both terms of equation (4). For TIP4P/2005 water models, they represent massless but charged site in the first summation and atoms in the second summation of the above equation. $K_C$, a and b denote electrostatic constant, and two different molecules, respectively. The H—H and H—O interactions between two different water molecules are ignored [43].

In this study, LAMMPS software [44] was used to execute the proposed EMD simulations. Particle-particle particle-mesh (PPPM) solver has been used for the long-range Coulombic interactions between charges [45]. The time step size was 0.001 ps. In our EMD simulation, the system was first relaxed under NVT (canonical) ensemble where the volume is fixed to ensure a given density at a certain temperature by using Nose–Hoover thermostat [46] for 20 ps. The system was then switched to NPT (constant pressure and temperature) ensemble using a Nose-Hoover barostat for 25 ps. Finally, NVE ensemble was used to maintain the constant energy and volume of the system for 60 ps before data collection starts. Fig. 1(c) shows the histories of the temperature and total energy of a 5 nm × 5 nm × 5 nm water cube simulated using the SPCE model. As can be seen from this figure, although the instantaneous temperature fluctuates around the targeted value of 300 k, the average temperature (dashed line) is maintained at 300 K. The total energy fluctuates before switching to NVE ensemble. However, it becomes constant when the system is under NVE ensemble. It should be noted that cases with longer running time for each stage were also tested and no noticeable changes in results were observed.

Fig. 2(a) shows a typical thermal conductivity and viscosity versus time curves in all three directions obtained using a 5 nm × 5 nm × 5 nm water cube with the SPCE model at T = 300 K. In this figure, K11, K22, and K33 represent the thermal conductivity in three directions while V11, V22, and V33 represent the viscosity in three directions. It can be seen that after a certain amount of time, both thermal conductivity and viscosity in each direction converge to a slightly different value. In terms of anisotropy, although the values are quite different in the beginning, they converge and become close to each other after a certain simulation time.

As already mentioned, in the conventional method of calculating thermal conductivity and viscosity, the property is determined by taking the average of a certain number of values from data points at different times after the autocorrelation function has converged to zero [47]. The major disadvantage of this method is that although the calculated properties converge in each simulation, the converged values are actually different in different simulations. In some studies, calculations of the properties are based on taking the average during the entire simulation time [30,48]. Overall, the conventional method of calculating the thermal conductivity and viscosity seems to have deficiency in the data sampling procedure.

This above issue can be clearly identified with a deeper look at the results of the following simulation case. Fig. 2(b) shows the data of the simulated thermal conductivity and viscosity collected between simulation time of 1000 ps and 2000 ps. Every single point in this graph is representing the average values of thermal conductivity or viscosity in three directions at the corresponding temperature over 2000 time steps (i.e. 2 ps). As can be seen from Fig. 2(b), although the target temperature is set to 300 K, it generally fluctuates from 295 to 305 during the simulation when the thermal conductivity and viscosity are being calculated. In addition, the instantaneous values of the simulated thermal conductivity and viscosity fluctuate.

Moreover, there is a deficiency in Fig. 2(b) as it is not able to clearly show the density of the dots because some dots might have overlapped each other if their values are very similar. As a result, contour plots are used to demonstrate the frequency of the data points as a function of the instantaneous temperature and thermophysical property value. Fig. 2(c) and (d) show the density plots of thermal conductivity and viscosity, respectively, of water simulated with SPCE water model at temperature T = 300 K for domain size of 5 nm. As can be seen from Fig. 2(c and d), the highest data density for both thermal conductivity and viscosity occurs at the temperature ranging from 298 K to 302 K.

Hence, it is not accurate to randomly pick one or a series of points from Fig. 2(b) and consider them as the thermal conductivity or viscosity of water at 300 K. It is thus proposed that the following key steps should be performed in order to obtain more reliable calculations of thermophysical properties of liquid using EMD simulations.

---

[1] For interpretation of color in Fig. 1, the reader is referred to the web version of this article.

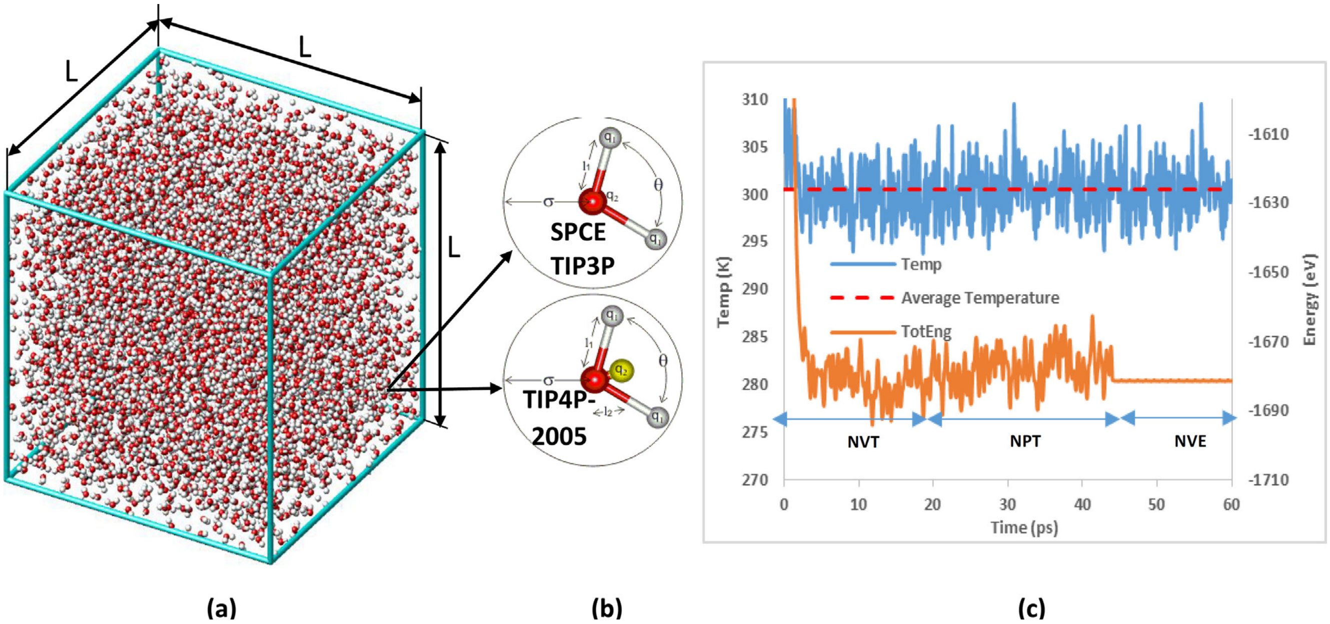

**Fig. 1.** (a) Schematic of the simulation domain with dimensions. (b) Configuration of the 3-site (SPC/E and TIP3P) and 4-site (TIP4P/2005) water models. (c) Fluctuations of temperature and total energy during the relaxation period obtained the SPC/E model.

**Table 1**
Parameters of water rigid models.

| Model | Type | σ, Å | ε, kJ/mol | r(OH), Å | r(OM), Å | qH (e) | qO (e) | qM (e) | HOH, deg |
|---|---|---|---|---|---|---|---|---|---|
| SPCE [27] | 3-site | 3.166 | 0.65 | 1 | N/A | 0.4238 | −0.8476 | – | 109.47 |
| TIP3P [26] | 3-site | 3.15061 | 0.6364 | 0.9572 | N/A | 0.417 | −0.834 | – | 104.52 |
| TIP4P/2005 [28] | 4-site | 3.1589 | 0.7749 | 0.9572 | 0.1546 | 0.5564 | – | −1.1128 | 104.52 |

- Step 1: In the EMD simulation of liquid, the system should be relaxed under NVT, NPT, and NVE ensembles for sufficiently long time (here, durations of 20 ps, 25 ps and 60 ps, respectively) so that no noticeable changes in results can be observed. The data collection process can then be started. During the production run of the EMD simulation, the instantaneous value of the thermophysical property in each direction will be obtained at every 2 ps using the GK formula. The average of the instantaneous values in the three directions at each time interval will then be taken and total of at least 1000 data points should be collected.
- Step 2: All the obtained results from Step 1 such as thermal conductivity (or viscosity) are grouped into 50 equal sets of data points with each set containing 20 data points. The standard deviations are calculated for each set of data points. The time history of the standard deviation of the simulated thermal conductivity (or viscosity) can then be plotted, as shown in Fig. 4(a and b).
- Step 3: Since the standard deviation calculated in Step 2 generally decreases with time, a cut-off time can be determined so that after this particular time point the standard deviation of the data set will be lower than a desired value. During the production run, only the data points after this cut-off time will be kept for further processing. For example, in this study it is observed from Fig. 4(a and b) that the standard deviation of the data set is constantly below 1% after 1000 ps of the production run. Therefore, only the data points collected after production run time of 1000 ps are used for further analysis and the data collected before 1000 ps are discarded.
- Step 4: In the vicinity of the target temperature, small-sized bins are defined to group the data which are within the small range of the target temperature (e.g. ± 8°). The size of the bin depends on the domain size and the range of the bins should be selected so that they can cover the regions with high data density as shown in Fig. 2(c and d).
- Step 5: The average value of the collected thermophysical property data in the bin containing the target temperature is calculated.
- Step 6: Steps 1–5 should be repeated for other independent EMD simulations with different initial particle velocity distribution generated using different random number seed. The total number of independent runs may vary at different studies based on the domain size, liquid properties, desired accuracy and so on. In this study, total of six independent EMD simulations are performed.
- Step 7: The average value of the thermophysical properties obtained from all the independent simulations will be considered as the final result of the simulated thermophysical property of the liquid.

In addition, in this study, the effect of the simulation box size and temperature are investigated by running simulations with different initial atomic velocity distribution for the three water models. Then, these results will be used to develop a guideline for selecting the size of the simulation box based on the desired standard deviation of the averaged thermophysical properties.

## 3. Results and discussion

### *3.1. Autocorrelation functions*

In Green-Kubo method, the accuracy of the calculated results is dependent on the total simulation time. At equilibrium of the simulation, the heat or stress current will still oscillate. As shown in Eqs. (2) and (3), Green-Kubo method strongly relies on how long it takes for the oscillations to become uncorrelated to the property (thermal conductivity or viscosity). Consequently, it is significant to find out when HACF or SACF decays to zero. Fig. 3(a) shows that HAFC is converging

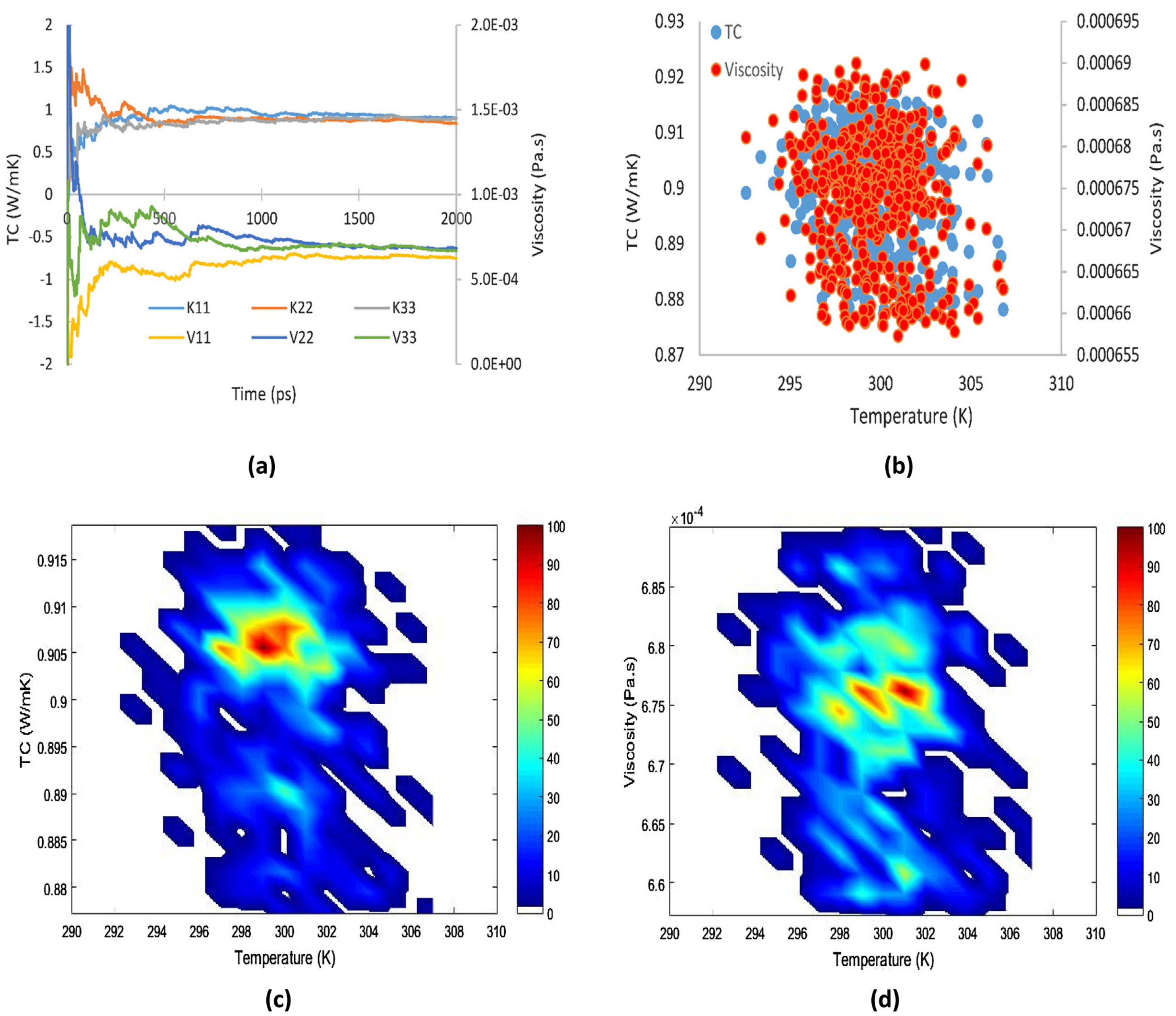

**Fig. 2.** (a) Typical thermal conductivity and viscosity curves (b) Thermal conductivity and viscosity values vs. temperature (c) Density plot of thermal conductivity and (d) density plot of viscosity values vs. temperature for an MD simulation with SPCE water model at T = 300 K.

to zero after about 40 ps from the start of calculating the thermal conductivity for the simulation of 5 nm × 5 nm × 5 nm water cube using SPCE model. However, as it is depicted in Fig. 3(b), SACF converges quickly to zero in less than 2 ps. It can be seen in this figure that autocorrelation function has a very rapid decay at the beginning followed by a trail that fluctuates slightly around zero. Such behaviour is the characteristic of the heat and stress autocorrelation functions while using Green-Kubo method to calculate thermophysical properties. In

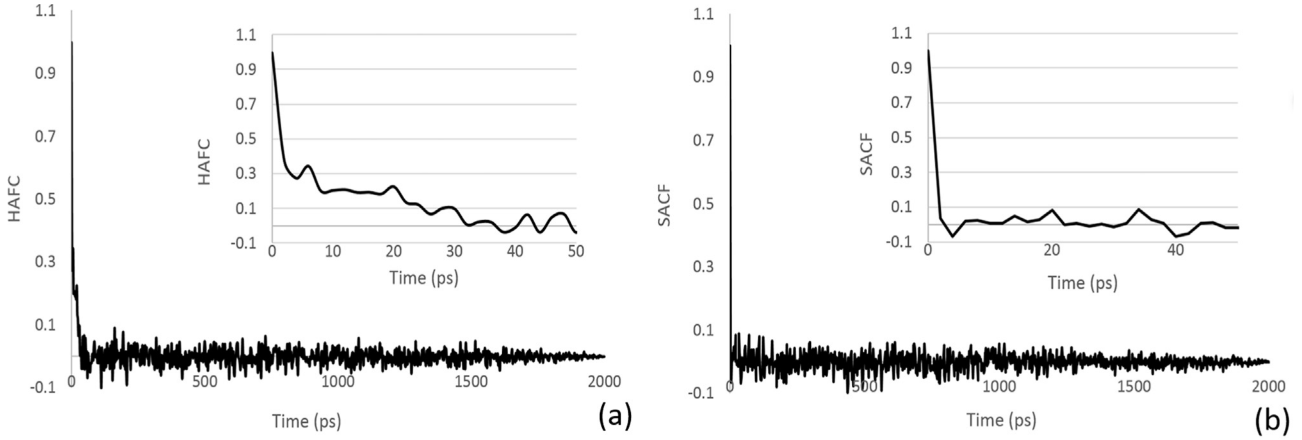

**Fig. 3.** HACF and SACF convergence for a SPCE water model at T = 300 K.

other words, not only it is a verification for EMD simulation using Green-Kubo formula, but also it shows that the simulation time (2000 ps) is large enough for this study as autocorrelation function reduces rapidly.

### 3.2. Error analysis of the simulation results

As it has been already shown in Fig. 2(a), the thermal conductivity and viscosity in each of the three directions will converge to an individual constant value after a certain amount of simulation time. However, a criterion needs to be defined to find the necessary simulation time after which the average of the obtained data can be regarded as the reliable estimation of the thermal conductivity and viscosity at the target temperature. The property is computed directly by performing a time integration of Eqs. (2) or (3) discussed in the methodology section. At the beginning of the simulation, there are too many fluctuations until the values start to converge. At this stage, it is crucial to introduce an approach of data processing in order to obtain the reliable results from the simulation data.

In this study, the thermophysical property values in the three directions simulated over 2000 ps are averaged at every 2 ps and then these data are divided into 50 equal sets (each set contains 20 data points). Afterward, the standard deviations are calculated for each aforementioned set of data. Fig. 4(a and b) shows the time histories of the standard deviation of thermal conductivity and viscosity simulated using SPCE water model with different simulation box size under temperature T = 300 K. A single dot in Fig. 4(a and b) represents the standard deviation of the thermal conductivity (Fig. 4(a)) and viscosity (Fig. 4(b)) for one data set. These calculations were repeated for different simulation boxes (L = 2 nm, 5 nm, 10 nm and 15 nm). It can be observed that after about 1000 ps simulation time, the standard deviations of both thermal conductivity and viscosity are below 1% regardless of the simulation box size. Hence, it is important to focus only on data collected between simulation time of 1000 ps and 2000 ps. Although Fig. 4(a and b) only illustrates the variation of standard deviation versus time for the simulated thermal conductivity and viscosity using SPCE water model at 300 K for four different simulation boxes, the behaviour of standard deviations are similar using TIP4P-2005 and TIP3P models.

In order to investigate the effect of the number of data points on the results, standard error of the estimated thermal conductivity and viscosity is calculated. Standard error demonstrated in Fig. 4(c and d) is for a single simulation with the box size of 10 nm and temperature of 300 K using SPCE water model. Over the simulation period of 1000 ps–2000 ps, simulation results were dumped at the time interval of 100 ps and 10,000 data points were obtained at each time interval. Thus, 106 data points were available in total. 100 datasets were formed each with randomly selected 10, 100, 1000, or the maximum 10,000 data points. Then, standard errors were calculated for each data set for each case as shown in Fig. 4(c and d). It can be seen that as the number of data points in a set of simulation increases, standard error decreases, indicating the improvement of the reliability.

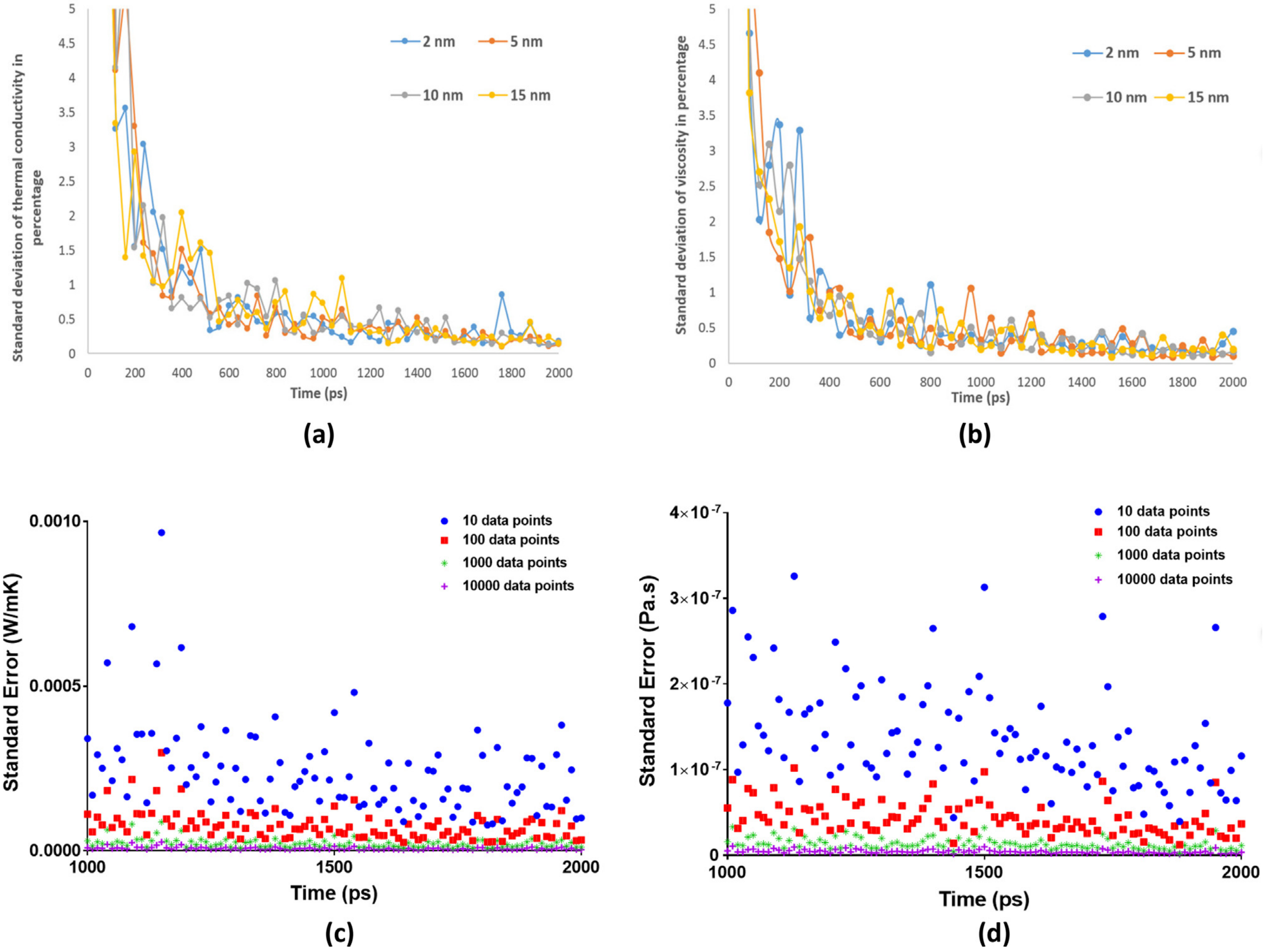

**Fig. 4.** Standard deviation of (a) thermal conductivity and (b) viscosity for different simulation boxes with SPCE water model at 300 K. Standard error of (c) thermal conductivity and (d) viscosity for a single simulation using SPCE water model at 300 K.

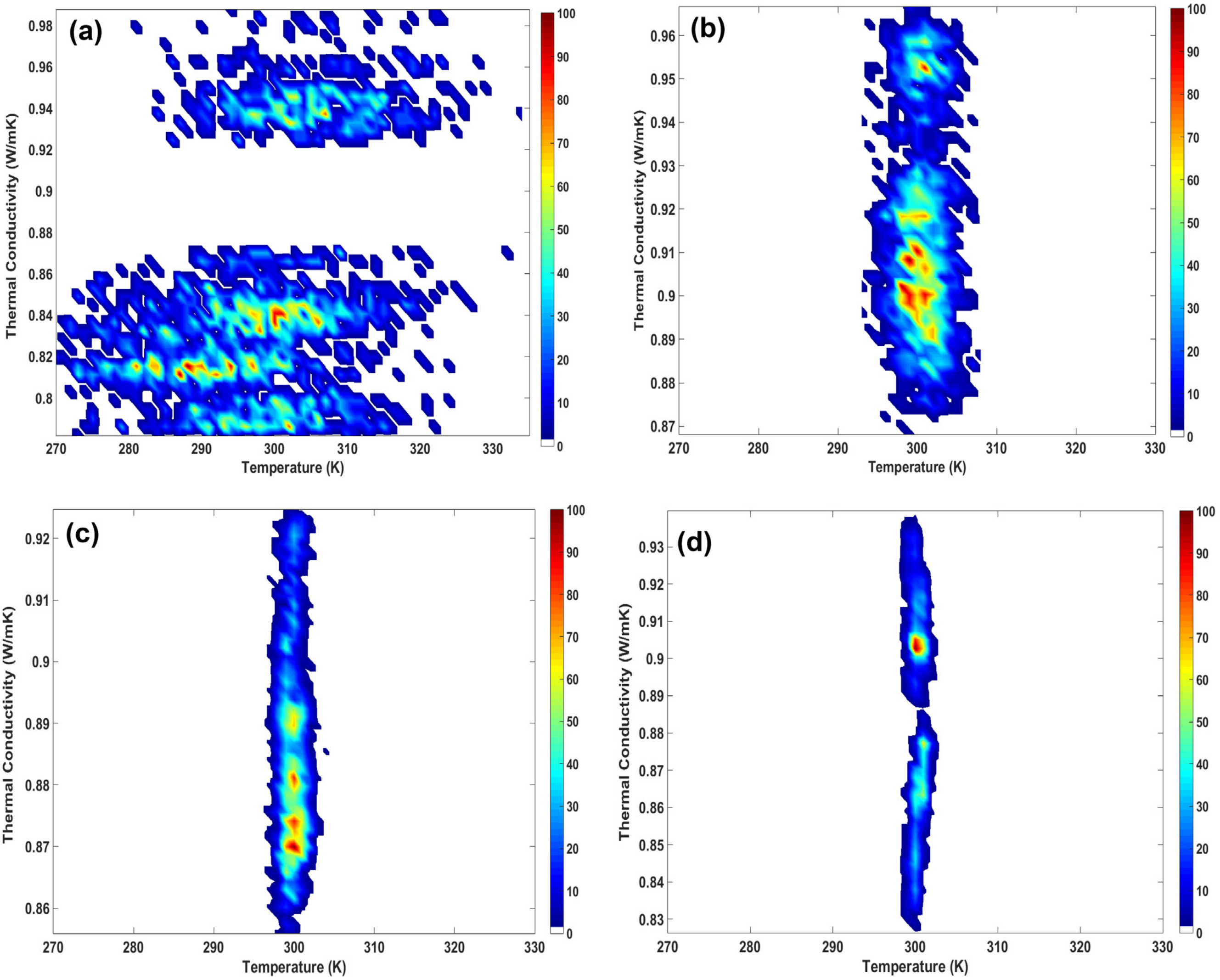

**Fig. 5.** Thermal conductivity mapping of SPCE water model versus temperature for domain size of (a) 2 nm, (b) 5 nm, (c) 10 nm, and (d) 15 nm.

### *3.3. Criteria for domain size selection*

In this part, the effects of simulation box size, water model and temperature on the thermal conductivity and viscosity are investigated. It is worth noting that the method of obtaining the thermal conductivity, viscosity and their standard deviations are the same as what was described in the methodology section. For all three water models, each simulation box was tested at four different temperatures including 290, 300, 310, and 320 K.

Fig. 5 shows the effect of the change in simulation box size on the thermal conductivity using SPCE water model. For all of these cases, the set temperature is 300 K. However, it can be seen that the distribution of the values of thermal conductivity can significantly vary by changing the size of the simulation box. These graphs also clearly show the importance of selecting proper bins for each case so as to focus on the regions with high data point density while eliminating the data that are relatively far from the target temperature. It can be seen that by increasing the size of the domain less scattered results can be obtained, which in turn reduces the standard deviation and increases the accuracy of the simulation.

Fig. 6 presents the density plot of viscosity for different simulation box sizes. Similar to the thermal conductivity, increase in simulation box size results in more concentrated results at the set temperature. Therefore, the obtained results are more reliable and accurate.

Fig. 7 is a quantitative performance evaluation of the new data processing method. It shows the effect of simulation box size on the standard deviation of the thermal conductivity and viscosity simulated at different temperatures for SPCE, TIP3P, and TIP4P-2005 models. It can be found from the figure that when the box size increases, the standard deviation of the simulated thermophysical properties decreases regardless of the simulation temperature and water model used.

It is worth noting that Fig. 7 also suggests a guideline, which could be used to design a simulation study. It can be seen that this guideline addresses the source of uncertainty in numerical simulations, i.e. domain size effect and its corresponding thermal gradient in the system. To choose the suitable domain size for more cost-effective simulations, the following guideline can be adopted. First, the target standard deviation and temperature of the system should be determined based on the requirements of the project. Second, the domain size can be determined by referring to Fig. 7 for a given water model.

In most of the cases, a relatively constant standard deviation is achieved at a given simulation temperature. However, it could be seen that in the viscosity simulation, the standard deviation increases by increasing the temperature with the domain size of 2 nm for SPCE and TIP3P models. Similar behaviour was observed in simulating thermal conductivity of TIP4P-2005 water model with the domain size of 2 nm. In addition, when TIP4P-2005 model is used in a 2 nm simulation box for calculating the viscosity of water, standard deviation decreases by increasing the temperature. All in all, it could be concluded that as has been discussed in Fig. 5(a) and Fig. 6(a), simulation box size of 2 nm is

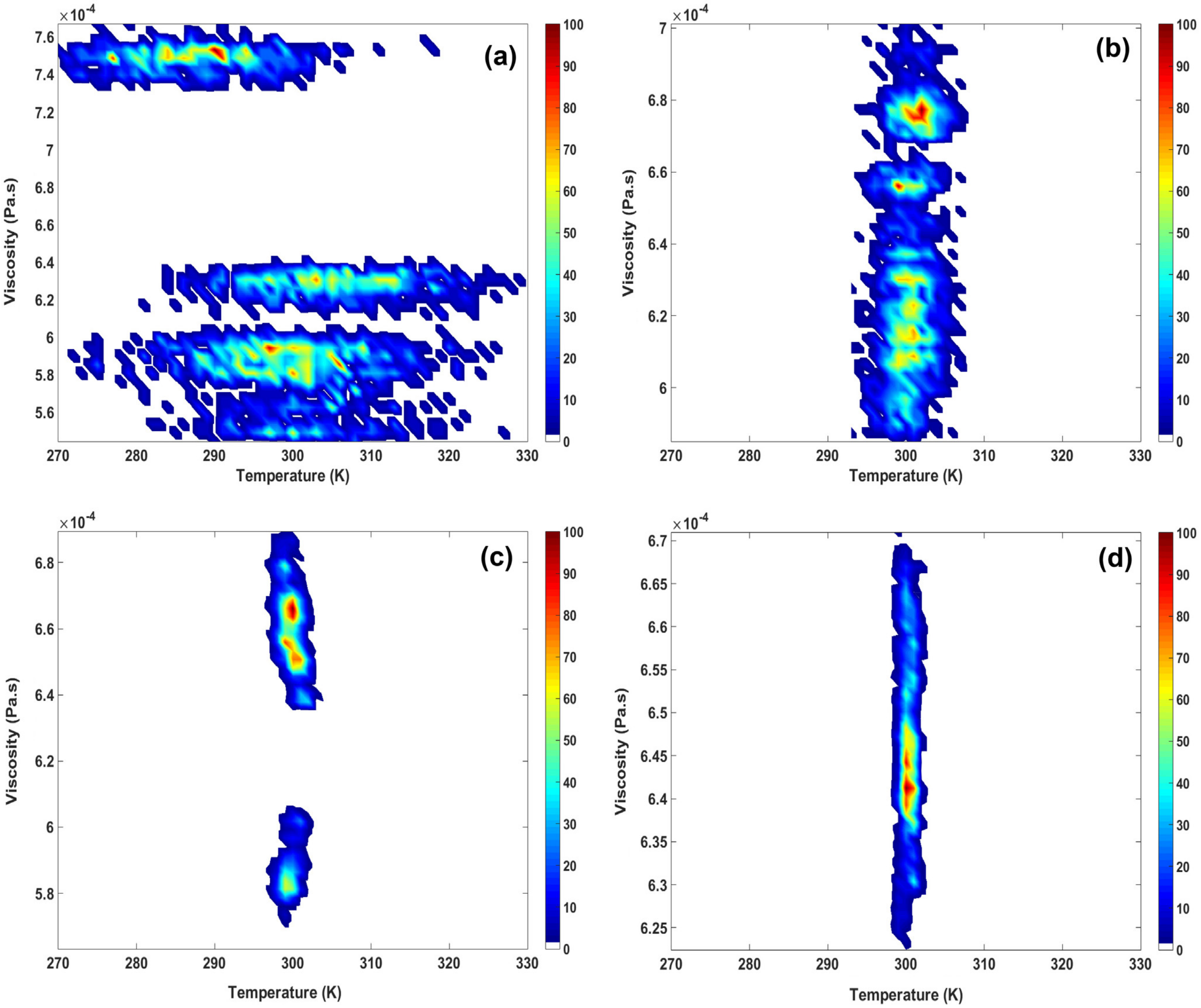

**Fig. 6.** Viscosity mapping of SPCE water model versus temperature for domain size of (a) 2 nm, (b) 5 nm, (c) 10 nm, and (d) 15 nm.

not appropriate for simulating thermophysical properties of water due to two reasons. Firstly, it results in very high standard deviations (around 10% for thermal conductivity and around 20% for viscosity). Secondly, standard deviation is varying substantially by changing the temperature in most cases.

These results can be used as a quantified guideline for MD simulation of the water. Indeed, the size of the simulation box could be selected based on the desired standard deviation for each specific simulation. For instance, for the SPCE water model, in order to have a standard deviation below 5%, the simulation box should be at least 5 nm. Whereas, if below 5% of standard deviation for viscosity calculation is expected, a box size of 10 nm or larger is required. The same interpretation could be used for the other two water models.

For thermal conductivity simulation, selecting domain sizes of 10 nm and 15 nm lead to standard deviation of 2% and 1%, respectively regardless of water model used. In terms of predicting viscosity, standard deviations increase to 4% and 2% with simulation box size of 10 nm and 15 nm, respectively.

## 4. Conclusion

In this study, a new data analysis procedure is proposed for calculating the thermal conductivity and viscosity using MD. In the proposed procedure, a simulation time after which the standard deviation of the values is below a given limit should be determined. Then, the average values of these data are calculated for 6 independent simulations with different initial atomic velocity distribution and the average result is reported as the property (thermal conductivity or viscosity). Based on the new approach, more reliable simulation data with controllable standard deviation can be obtained. It should be noted that, although this study is based on EMD simulation, the introduced approach could be applicable to NEMD simulations as well.

Furthermore, this study has demonstrated that the simulation box size is an important parameter and should be carefully investigated in the MD simulations of thermophysical properties. Moreover, due to the nature of GK calculation, the deviation of thermophysical values caused by the artificial self-correlations is addressed. Then, the common method of mitigating this problem, i.e. increasing domain size, has been systematically studied to introduce a quantified guideline, which could be used accordingly based on the accuracy requirements of a simulation task.

As an example of using the proposed guideline, the standard deviation of the thermal conductivity and viscosity simulations for three water models is calculated using the new approach. It has been shown that in order to obtain accurate and reliable thermophysical properties of water with standard deviation of below 5%, the simulation box size

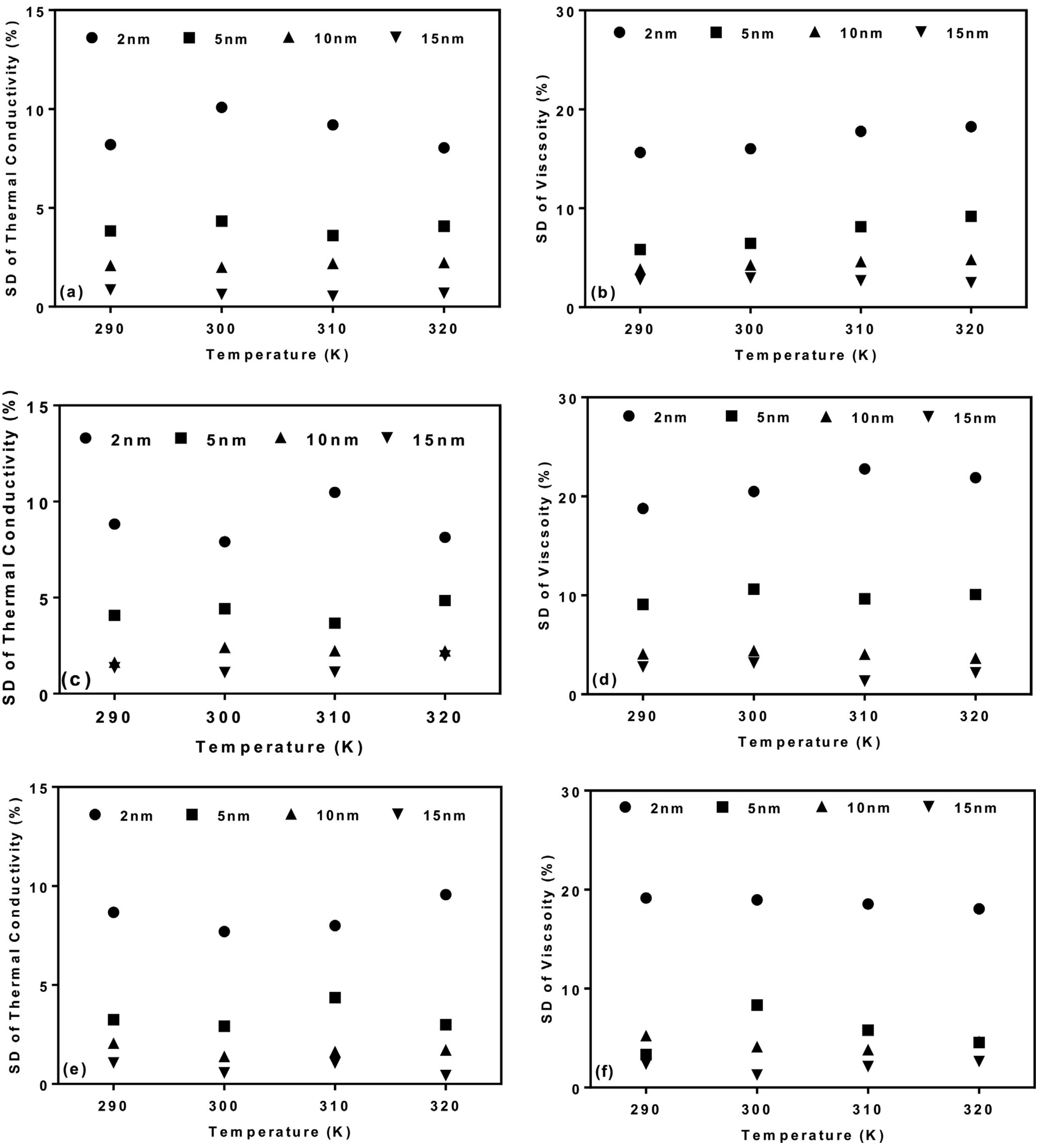

**Fig. 7.** Standard deviation of thermal conductivity (left) and viscosity (right) vs. temperature for different simulation boxes using (a), (b) SPCE; (c), (d) TIP3P; and (e), (f) TIP4P-2005 water model.

should be at least $5 \times 5 \times 5\,\mathrm{nm}^3$ and $10 \times 10 \times 10\,\mathrm{nm}^3$ to simulate thermal conductivity and viscosity of water, respectively.

## Acknowledgments

This work was financially supported in part by the Australian Research Council through Discovery Projects (DP170102886) and by the National Natural Science Foundation of China (Grant No. 11232003). This research was undertaken with the assistance of resources and services from the National Computational Infrastructure (NCI), which is supported by the Australian Government.

## Appendix A. Supplementary material

Supplementary data to this article can be found online at https://doi.org/10.1016/j.cplett.2018.09.048.

## References

[1] G. Karniadakis, A. Beskok, N. Aluru, Microflows and Nanoflows: Fundamentals and

Simulation, Springer Science & Business Media, 2006.
[2] M. Kim, D. Ha, T. Kim, Cracking-assisted photolithography for mixed-scale patterning and nanofluidic applications, Nat. Commun. (2015) 6.
[3] S.M.S. Murshed, K.C. Leong, C. Yang, Enhanced thermal conductivity of $TiO_2$—water based nanofluids, Int. J. Therm. Sci. 44 (4) (2005) 367–373.
[4] Z. Zhang, Nano/Microscale Heat Transfer, McGraw-Hill Education, 2007.
[5] E.B. Haghighi, M. Saleemi, N. Nikkam, Z. Anwar, I. Lumbreras, M. Behi, S.A. Mirmohammadi, H. Poth, R. Khodabandeh, M.S. Toprak, M. Muhammed, B. Palm, Cooling performance of nanofluids in a small diameter tube, Exp. Therm Fluid Sci. 49 (2013) 114–122.
[6] E.W. Lemmon, R.T. Jacobsen, Viscosity and thermal conductivity equations for nitrogen, oxygen, argon, and air, Int. J. Thermophys. 25 (1) (2004) 21–69.
[7] T.Q. Vo, B. Kim, Transport phenomena of water in molecular fluidic channels, Sci. Rep. 6 (2016) 33881.
[8] M. Javanmardi, K. Jafarpur, A molecular dynamics simulation for thermal conductivity evaluation of carbon nanotube-water nanofluids, J. Heat Trans. 135 (4) (2013) 042401.
[9] W. Duangthongsuk, S. Wongwises, Measurement of temperature-dependent thermal conductivity and viscosity of $TiO_2$-water nanofluids, Exp. Therm. Fluid Sci. 33 (4) (2009) 706–714.
[10] P. Cosenza, R. Guérin, A. Tabbagh, Relationship between thermal conductivity and water content of soils using numerical modelling, Eur. J. Soil Sci. 54 (3) (2003) 581–588.
[11] S. Volz, J.B. Saulnier, G. Chen, P. Beauchamp, Computation of thermal conductivity of Si/Ge superlattices by molecular dynamics techniques, Microelectron. J. 31 (9) (2000) 815–819.
[12] M.-S. Jeng, R. Yang, D. Song, G. Chen, Modeling the thermal conductivity and phonon transport in nanoparticle composites using Monte Carlo simulation, J. Heat Transfer 130 (4) (2008) 042410.
[13] G. Puliti, S. Paolucci, M. Sen, Thermodynamic properties of gold–water nanofluids using molecular dynamics, J. Nanopart. Res. 14 (12) (2012) 1–14.
[14] W. Cui, Z. Shen, J. Yang, S. Wu, Effect of chaotic movements of nanoparticles for nanofluid heat transfer augmentation by molecular dynamics simulation, Appl. Therm. Eng. 76 (2015) 261–271.
[15] V. Vijayaraghavan, C. Wong, Transport characteristics of water molecules in carbon nanotubes investigated by using molecular dynamics simulation, Comput. Mater. Sci. 89 (2014) 36–44.
[16] H. Kang, Y. Zhang, M. Yang, L. Li, Nonequilibrium molecular dynamics simulation of coupling between nanoparticles and base-fluid in a nanofluid, Phys. Lett. A 376 (4) (2012) 521–524.
[17] G. Lu, Y.-Y. Duan, X.-D. Wang, Surface tension, viscosity, and rheology of water-based nanofluids: a microscopic interpretation on the molecular level, J. Nanopart. Res. 16 (9) (2014) 2564.
[18] T. Akiner, H. Ertürk, K. Atalik, Prediction of Thermal Conductivity and Shear Viscosity of Water-Cu Nanofluids Using Equilibrium Molecular Dynamics, ASME 2013 International Mechanical Engineering Congress and Exposition, American Society of Mechanical Engineers, 2013.
[19] P.K. Schelling, S.R. Phillpot, P. Keblinski, Comparison of atomic-level simulation methods for computing thermal conductivity, Phys. Rev. B 65 (14) (2002) 144306.
[20] M.S. Green, Markoff random processes and the statistical mechanics of time--dependent phenomena. II. irreversible processes in fluids, J. Chem. Phys. 22 (3) (1954) 398–413.
[21] R. Kubo, Statistical-mechanical theory of irreversible processes. I. general theory and simple applications to magnetic and conduction problems, J. Phys. Soc. Jpn. 12 (6) (1957) 570–586.
[22] M. Caro, L.K. Béland, G.D. Samolyuk, R.E. Stoller, A. Caro, Lattice thermal conductivity of multi-component alloys, J. Alloy. Compd. 648 (2015) 408–413.
[23] B. Guillot, A reappraisal of what we have learnt during three decades of computer simulations on water, J. Mol. Liq. 101 (1) (2002) 219–260.
[24] M.A. González, J.L. Abascal, The shear viscosity of rigid water models, J. Chem. Phys. 132 (9) (2010) 096101.
[25] W.L. Jorgensen, J. Chandrasekhar, J.D. Madura, R.W. Impey, M.L. Klein, Comparison of simple potential functions for simulating liquid water, J. Chem. Phys. 79 (2) (1983) 926–935.
[26] M.W. Mahoney, W.L. Jorgensen, A five-site model for liquid water and the reproduction of the density anomaly by rigid, nonpolarizable potential functions, J. Chem. Phys. 112 (20) (2000) 8910–8922.
[27] P.G. Kusalik, I.M. Svishchev, The spatial structure in liquid water, Science (Washington) 265 (5176) (1994) 1219–1221.
[28] J.L.F. Abascal, C. Vega, A general purpose model for the condensed phases of water: TIP4P/2005, J. Chem. Phys. 123 (23) (2005) 234505.
[29] Y. Mao, Y. Zhang, Thermal conductivity, shear viscosity and specific heat of rigid water models, Chem. Phys. Lett. 542 (2012) 37–41.
[30] X. Zhang, Y. Gao, Y. Chen, M. Hu, Robustly engineering thermal conductivity of bilayer graphene by interlayer bonding, Sci. Rep. 6 (2016) 22011.
[31] T. Akıner, J. Mason, H. Ertürk, Thermal characterization assessment of rigid and flexible water models in a nanogap using molecular dynamics, Chem. Phys. Lett. 687 (2017) 270–275.
[32] N.J. English, J.S. Tse, Thermal conductivity of supercooled water: an equilibrium molecular dynamics exploration, J. Phys. Chem. Lett. 5 (21) (2014) 3819–3824.
[33] D. Bedrov, G.D. Smith, Thermal conductivity of molecular fluids from molecular dynamics simulations: application of a new imposed-flux method, J. Chem. Phys. 113 (18) (2000) 8080–8084.
[34] P. Kumar, H.E. Stanley, Thermal conductivity minimum: a new water anomaly, J. Phys. Chem. B 115 (48) (2011) 14269–14273.
[35] L. Shen, Z. Chen, Molecular dynamics study of the specimen size and imperfection effects on the failure responses of multi-nanobar structures, Int. J. Multiscale Comput. Eng. 8 (2) (2010).
[36] C. Chen, L. Shen, M. Ma, J.Z. Liu, Q. Zheng, Brownian motion-induced water slip inside carbon nanotubes, Microfluid. Nanofluid. 16 (1–2) (2014) 305–313.
[37] M.G. Muraleedharan, D.S. Sundaram, A. Henry, V. Yang, Thermal conductivity calculation of nano-suspensions using Green-Kubo relations with reduced artificial correlations, J. Phys.: Condens. Matter 29 (15) (2017) 155302.
[38] S. Stackhouse, L. Stixrude, Theoretical methods for calculating the lattice thermal conductivity of minerals, Rev. Mineral. Geochem. 71 (1) (2010) 253–269.
[39] T.L. Bergman, F.P. Incropera, D.P. DeWitt, A.S. Lavine, Fundamentals of Heat and Mass Transfer, John Wiley & Sons, 2011.
[40] R. Vogelsang, C. Hoheisel, G. Ciccotti, Thermal conductivity of the Lennard-Jones liquid by molecular dynamics calculations, J. Chem. Phys. 86 (11) (1987) 6371–6375.
[41] W.G. Hoover, D.J. Evans, R.B. Hickman, A.J. Ladd, W.T. Ashurst, B. Moran, Lennard-Jones triple-point bulk and shear viscosities. Green-Kubo theory, Hamiltonian mechanics, and nonequilibrium molecular dynamics, Phys. Rev. A 22 (4) (1980) 1690.
[42] S.C.P.C.H. COCHRAN, The calculation of viscosity of liquid n-decane and n-hexadecane by the Green-Kubo method, Mol. Phys. 93 (1) (1998) 117–122.
[43] J.E. Jones, On the Determination of Molecular Fields. II. From the Equation of State of a Gas, Proc. R. Soc. Lond. Ser. A 106 (738) (1924) 463–477.
[44] S. Plimpton, Fast parallel algorithms for short-range molecular dynamics, J. Comput. Phys. 117 (1) (1995) 1–19.
[45] R.W. Hockney, J.W. Eastwood, Computer simulation using particles, crc Press, 1988.
[46] W.G. Hoover, Canonical dynamics: equilibrium phase-space distributions, Phys. Rev. A 31 (3) (1985) 1695.
[47] J. Moon, A.J. Minnich, Sub-amorphous thermal conductivity in amorphous heterogeneous nanocomposites, RSC Adv. 6 (107) (2016) 105154–105160.
[48] X. Qian, X. Gu, R. Yang, Lattice thermal conductivity of organic-inorganic hybrid perovskite $CH_3NH_3PbI_3$, Appl. Phys. Lett. 108 (6) (2016) 063902.